

Article

Hydrochemical Characteristics and Formation Mechanism of Strontium-Rich Groundwater in Tianjiazhai, Fugu, China

Chengcheng Liang^{1,2}, Wei Wang^{1,2,*}, Xianmin Ke^{1,2}, Anfeng Ou^{1,2} and Dahao Wang^{1,2}

¹ School of Water and Environment, Chang'an University, No. 126 Yanta Road, Xi'an 710054, China; 2020129022@chd.edu.cn (C.L.); 2020029009@chd.edu.cn (X.K.); 2020129020@chd.edu.cn (A.O.); 2018129018@chd.edu.cn (D.W.)

² Key Laboratory of Subsurface Hydrology and Ecological Effects in Arid Region, Chang'an University, Ministry of Education, No. 126 Yanta Road, Xi'an 710054, China

* Correspondence: wangweichd@chd.edu.cn

Abstract: Strontium-rich groundwater exists in the underlying carbonate rocks of the Tianjiazhai Shimachuan River basin, Fugu, China. In this study, the hydrochemical characteristics and formation mechanisms of Sr-rich groundwater were assessed using mathematical statistics and traditional water chemistry, combining geological and hydrogeological conditions, as well as hydrogeochemical theory. The results showed that the Sr²⁺ content range in Sr-rich groundwater was 0.85~2.99 mg·L⁻¹, which is weakly alkaline fresh water. HCO₃⁻·Ca·Mg·Na was the main facies type of Sr-rich groundwater. Sr-rich groundwater has relatively stable contents of chemical elements. The water–rock interaction was the main factor controlling the hydrochemical characteristics of Sr-rich groundwater, particularly carbonate dissolution, influenced by some degree of cation exchange. The Sr element in groundwater mainly comes from the dissolution of the sandstone of the Yanchang Formation. The higher the degree of weathering and the longer the water–rock reaction time, the more favorable the dissolution and enrichment of Sr in groundwater. Moreover, the large weathering thickness and fracture development of the rocks in the Tianjiazhai area provide favorable conditions for the formation of Sr-rich groundwater. The results of this study provide a scientific basis for developing effective policies to protect Sr-rich groundwater resources.

Keywords: strontium-rich groundwater; hydrochemical characteristics; formation mechanisms; hydrogeochemistry



Citation: Liang, C.; Wang, W.; Ke, X.; Ou, A.; Wang, D. Hydrochemical Characteristics and Formation Mechanism of Strontium-Rich Groundwater in Tianjiazhai, Fugu, China. *Water* **2022**, *14*, 1874. <https://doi.org/10.3390/w14121874>

Academic Editors: Thomas Meixner and Elias Dimitriou

Received: 4 May 2022

Accepted: 8 June 2022

Published: 10 June 2022

Publisher's Note: MDPI stays neutral with regard to jurisdictional claims in published maps and institutional affiliations.



Copyright: © 2022 by the authors. Licensee MDPI, Basel, Switzerland. This article is an open access article distributed under the terms and conditions of the Creative Commons Attribution (CC BY) license (<https://creativecommons.org/licenses/by/4.0/>).

1. Introduction

As an important source of water supply for human beings and an important component of the hydrological cycle, groundwater is of great importance for the sustainable development of the socio-economy and the protection of ecological stability [1,2]. Groundwater hydrochemical characteristics are controlled by natural and anthropogenic factors and are the result of long-term interactions between groundwater and the environment. Therefore, hydrochemical analysis of groundwater can reveal the hydrochemical formation mechanisms [3,4]. In natural conditions, the hydrochemical characteristics of groundwater are mainly controlled by dissolution, concentration, desulfation/carbonation, cation exchange, and mixing processes [5,6]. However, various changes in the hydrochemical characteristics of groundwater may occur under the influence of anthropogenic activities [7,8]. Under natural conditions, elements in rock layers are enriched into groundwater by hydrogeochemical processes, which can lead to mineralization and contamination of groundwater [9]. For example, under natural conditions, large amounts of dissolution of soluble rocks (carbonate rocks) can lead to mineralization of groundwater. In addition, trace elements (arsenic and fluorine) may be enriched to levels threatening human health under natural hydrogeochemistry [10,11]. A series of groundwater pollution problems have emerged under the influence of human activities, such as nitrate pollution of groundwater.

Multivariate statistical analysis and hydrogeochemistry are often used to investigate the hydrochemical characteristics of groundwater and their determining factors [12]. Recent studies on groundwater hydrochemistry have used a combination of several methods (mathematical statistics, water chemistry, hydrogeochemical simulation, etc.) to assess the hydrochemical characteristics of groundwater [13–15].

Strontium (Sr) is one of the essential trace elements for human health, which maintains human physiological functions [16,17]. Strontium in groundwater is derived from Sr in the surrounding rock and enters the groundwater through a leaching process via infiltration of atmospheric precipitation [18,19]. Suitable hydrogeological conditions are the basic conditions for the formation of strontium-rich groundwater. In fact, the extent of Sr-enrichment in the groundwater depends on the hydrogeochemical processes occurring in aquifers [20]. The amount of Sr in the surrounding rock entering the groundwater system is positively correlated with the degree of rock weathering. In addition, CO₂ content, temperature, and redox conditions are the important factors affecting the Sr enrichment in groundwater [21]. The Sr abundance in the surrounding rocks determines the Sr content in groundwater. Long-distance runoff and long-path circulation of groundwater increase the water–rock reaction time, thus promoting strontium enrichment [22]. The formation of Sr-rich groundwater is controlled by tectonic magmatic activity, Sr content in surrounding rocks, and hydrogeochemical conditions [23]. In recent years, numerous researchers have devoted considerable attention to the formation mechanism and enrichment factors of Sr in groundwater [24–26].

Fugu County is located in the Loess Plateau area in Northwest China, where surface water resources are limited. Indeed, groundwater has long been the source of local water supply in the area. However, in recent years, with the exploitation of coal resources and the development of the industrial economy, groundwater resource in Fugu County has become overexploited and inefficient. In the Shimachuan River basin in the Tianjiazhai area of Fugu County, Sr-rich groundwater exists in the underlying carbonate strata. The population of Shimachuan River Basin is 10,647 people, and the main water source for the production and living of local residents is groundwater. However, there are few studies on the hydrochemical characteristics and formation mechanism of Sr-rich groundwater in this area. Therefore, in this study, the hydrochemical characteristics of Sr-rich groundwater and its formation mechanism were assessed using descriptive analyses, Piper trilinear diagrams, Gibbs plots, ionic ratios, and correlation analysis. In addition, the formation conditions of Sr in groundwater were analyzed by combining geological and hydrogeological conditions as well as hydrogeochemical theory to reveal the formation mechanism of Sr in groundwater.

2. Materials and Methods

2.1. Study Area

The study area is located in the Shimachuan River basin of Fugu County in the eastern part of the Loess Plateau in North Shaanxi in China, belonging to the typical semi-arid continental monsoon climate (Figure 1). The terrain of the study area is generally high in the west and low in the east, with elevations ranging from 940 m to 1100 m. The geomorphology of the study area mainly consists of Loess mountains and river valley terraces. Loess mountains are mainly distributed on both sides of Shimachuan valley, with an elevation of 1000~1100 m and a width of 100~250 m, and incline to both sides of the valley at a slope angle of 10~20°. The Loess peak is narrow, along the watershed there are large ups and downs, and the ground is very broken, forming a unique Loess landform. The Loess Mountain area has uniform lithology, good water permeability, small catchment area and serious soil erosion. Valley terraces are mainly distributed along the Shimachuan river, with an elevation of 960~1100 m. The valley terraces are long, sporadic and intermittent. The area of the valley terraces is small. The front edge of the valley terraces is 2~3 m higher than the river bed, 15~40 m wide, and most of the terraces tilt to the river bed at a slope angle of 3~5°. The overall surface water network is poorly developed in the study area. The Shimachuan River in the study area is a first-class tributary of the west bank of the Yellow

River. In addition, groundwater is the main water supply source in the study area, stored at the bottom of the Quaternary formation and in bedrock fissures. Sr-rich groundwater in the study area is mainly stored in the weathered and fractured aquifer (unconfined) of the Yanchang Formation. Its recharge mainly occurs from atmospheric precipitation and the unconfined water of the loose layer of the Quaternary formation and surface water, which eventually discharges at the downstream outlet of the Shimachuan River. The stratigraphy of the Yanchang formation is covered by loose sediments of the Quaternary formation, with outcrops in the river valley; the thickness of strata is 200~411 m, the maximum exposed thickness is 65 m, and the thickness of the weathering layer is 20~43.26 m. In addition, the lithology of the Yanchang formation consists of a thickly laminated light gray-green medium to fine-grained feldspathic sandstone with medium sorting and roundness. It has large inclined beddings, wedge-shaped beddings and massive beddings. The study area is located in the northeast of the secondary tectonic units of Ordos Basin, with stable geological structures and oscillatory rise caused by the neotectonic movement. There is no trace of magmatic activity in the area. The overall structure is monoclinical with a dip direction of 292° and a dip angle of 1~4°.

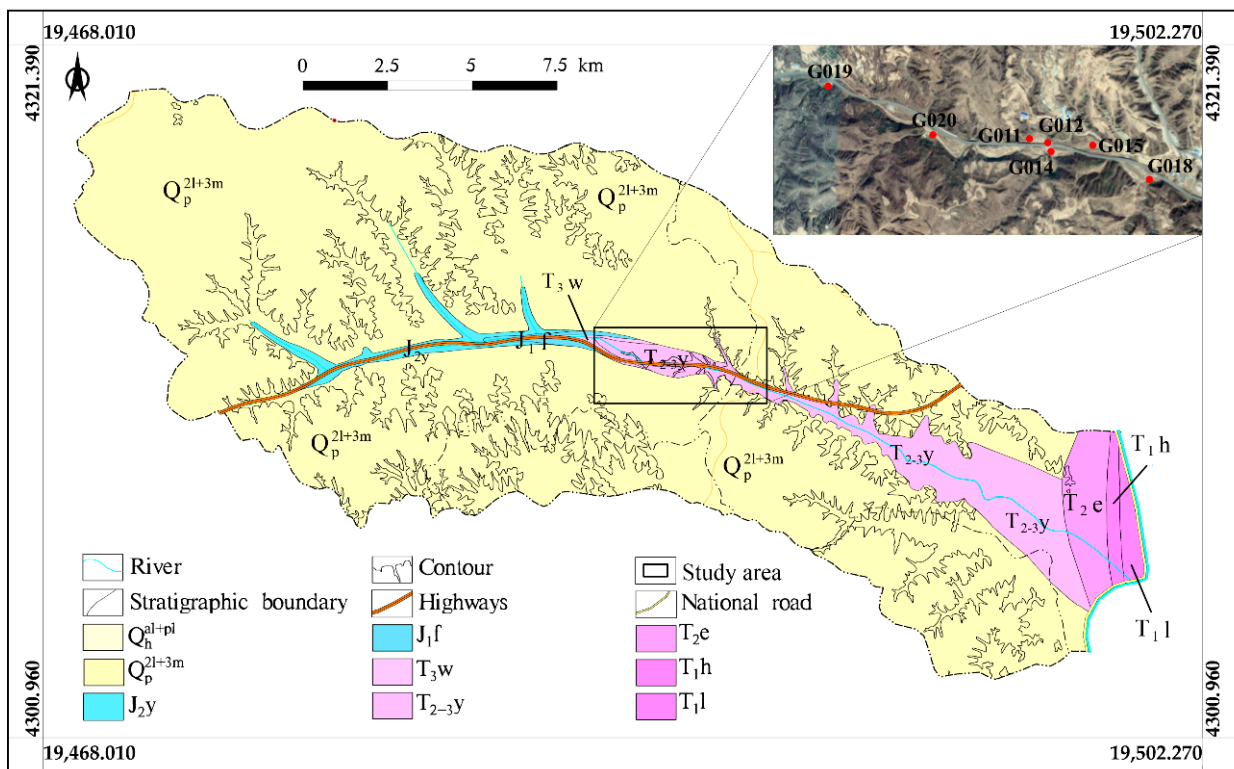


Figure 1. Regional geological map of Tianjiazhai East Ditch, Fugu County. The geographical location of the study area belongs to the 19th projection band of the Gaussian projection six-degree band, and the coordinates used in the figure are the Gaussian projection six-degree band coordinate system.

2.2. Sampling

In this study, 30 groundwater samples were first collected from hydrogeological boreholes in the study area during the March 2018 to September 2019 period, according to the Technical Requirements for Water Sample Collection and Delivery issued by the China Geological Survey. These were then analyzed for groundwater quality, the test indexes including pH, total dissolved solids (TDS), total hardness, cation (K^+ , Na^+ , Ca^{2+} and Mg^{2+}), anion (Cl^- , HCO_3^- , SO_4^{2-} and NO_3^-) and strontium elements. The rock type of the sampling point was sandstone of Yanchang Formation. In addition, 25 and 24 rock samples were collected at different depths from drilling G019 and G020 in the study area,

respectively, while 22 rock samples were collected from a selected profile between drilling G020 and the Temple River Gully. All the rock samples were analyzed for Sr content.

2.3. Methods

The pH value was determined by water quality tester (SD150), the total dissolved solids (TDS) was determined by gravimetric method (GR), the total hardness was determined by ethylene diamine tetraacetic acid disodium titration, and the contents of cations K^+ , Na^+ , Ca^{2+} and Mg^{2+} were determined by atomic absorption spectrometer (ICP-AES) [27–29]. The contents of anions Cl^- , SO_4^{2-} and NO_3^- were determined by ion chromatograph (IC-90), and HCO_3^- was determined by hydrochloric acid titration [30,31]. Sr^{2+} was determined by plasma mass spectrometry (ICP-MS). The content of strontium (Sr) in rock was determined by EDTA volumetric method [32,33]. The free carbon dioxide in groundwater was determined by the volumetric method of standard alkali solution [34].

In this study, the descriptive statistics of physicochemical parameters of groundwater were performed using SPSS 22.0 software. Mineral saturation indexes (SI) were calculated by hydrochemical simulation software Phreeqc, and the database was the phreeqc.dat thermodynamic database [35]. Pearson correlation analysis was performed to evaluate the relationship between physicochemical parameters of groundwater. In addition, groundwater chemical types were classified using the Shukarev classification method and Piper trilinear diagram, while the main controlling factors of groundwater chemistry in the study area were determined using the Gibbs diagram. The main ion sources of Sr-rich groundwater were studied using ionic ratio diagrams. The formation mechanism of Sr in groundwater was investigated based on the geological and hydrogeological conditions as well as hydrogeochemical theory.

3. Results and Discussion

3.1. Hydrochemical Characteristics

3.1.1. Descriptive Analysis of Hydrochemical Characteristics

As reported in Table 1, the Sr^{2+} content in Sr-rich groundwater in the study area ranged from 0.85 to 2.99 $mg \cdot L^{-1}$, with a mean value of 1.45 $mg \cdot L^{-1}$, which is 7.25 times higher than the national limit value of Sr^{2+} content in natural mineral water for drinking (0.20 $mg \cdot L^{-1}$). Compared with Sr^{2+} content in Sr-rich groundwater in other areas of China, the Sr^{2+} content in groundwater in the study area is close to that in Xintian County of Hunan Province (1.57 $mg \cdot L^{-1}$), and lower than that in Guanling area of Guizhou Province (2.43 $mg \cdot L^{-1}$). The Sr^{2+} content in groundwater in the study area is higher than that in Changchun, Jilin province (0.29 $mg \cdot L^{-1}$), Xianning, Hubei Province (0.63 $mg \cdot L^{-1}$), Yutian county, Xinjiang Province (1.1 $mg \cdot L^{-1}$) and Pingxiang city, Jiangxi Province (1.29 $mg \cdot L^{-1}$). Sr-rich groundwater pH range was 7.50–8.30, with an average value of 7.92, indicating a slightly alkaline Sr-rich groundwater. Part of the water samples in the study had a high PH value of 8.3, mainly because there was a little amount of CO_3^{2-} in the groundwater. CO_3^{2-} will combine with H^+ in water, leading to the decrease of hydrogen ion concentration in groundwater. The pH value of Sr-rich groundwater meets the requirements of the Chinese Standards (6.5–8.5) and the WHO Guidelines (6.5–8.5). TDS (total dissolved solids) ranged from 332 to 718 $mg \cdot L^{-1}$, with a mean value of 492.57 $mg \cdot L^{-1}$, showing low TDS levels in Sr-rich groundwater. The total hardness ranged from 205.00 to 825.00 $mg \cdot L^{-1}$, with a mean value of 324.90 $mg \cdot L^{-1}$, suggesting medium-hard and ultra-hard water. The TDS of Sr-rich groundwater meets the requirements of the Chinese Standards (1000 $mg \cdot L^{-1}$) and the WHO Guidelines (1000 $mg \cdot L^{-1}$). The dominant cations in Sr-rich groundwater were Ca^{2+} , Na^+ , and Mg^{2+} , with average contents of 71.09, 60.57, and 31.77 $mg \cdot L^{-1}$, accounting for 42.73, 36.41, and 19.10% of total cation contents, respectively, whereas K^+ showed the lowest content in Sr-rich groundwater, with an average value of 2.92 $mg \cdot L^{-1}$, accounting for only 1.76% of total cation contents. The Na^+ content of Sr-rich groundwater is lower than the maximum Na^+ content required by the Chinese Standards (200 $mg \cdot L^{-1}$) and the WHO Guidelines (200 $mg \cdot L^{-1}$). On the other hand, HCO_3^- was the dominant anion in

Sr-rich groundwater, with mean values of $348.80 \text{ mg}\cdot\text{L}^{-1}$, accounting for 73.52% of total anion contents, whereas NO_3^- showed the lowest content in Sr-rich groundwater, with an average value of $7.76 \text{ mg}\cdot\text{L}^{-1}$, accounting for only 1.63% of total anion contents. The Cl^- content of Sr-rich groundwater is lower than the maximum Cl^- content required by the Chinese Standards ($250 \text{ mg}\cdot\text{L}^{-1}$) and the WHO Guidelines ($250 \text{ mg}\cdot\text{L}^{-1}$). The SO_4^{2-} content of Sr-rich groundwater is lower than the maximum SO_4^{2-} content required by the Chinese Standards ($250 \text{ mg}\cdot\text{L}^{-1}$) and the WHO Guidelines ($500 \text{ mg}\cdot\text{L}^{-1}$). The NO_3^- content of Sr-rich groundwater is lower than the maximum NO_3^- content required by the WHO Guidelines ($50 \text{ mg}\cdot\text{L}^{-1}$) and higher than the maximum NO_3^- content required by the Chinese Standards ($20 \text{ mg}\cdot\text{L}^{-1}$). This is due to the agricultural activities of local residents in the study area, resulting in the increase of NO_3^- content. The coefficients of variation of the hydrochemical parameters of Sr-rich groundwater were all less than 1, indicating relatively stable contents of these hydrochemical components in Sr-rich groundwater. This finding may be due primarily to the fact that Sr-rich groundwater in the study area is strongly controlled by geological conditions and less influenced by human activities.

Table 1. Statistics on the hydrochemical characteristics of Sr-rich groundwater.

Projects	$\text{mg}\cdot\text{L}^{-1}$											pH
	K^+	Na^+	Ca^{2+}	Mg^{2+}	Cl^-	SO_4^{2-}	HCO_3^-	NO_3^-	Sr^{2+}	TH *	TDS	
Min	1.63	33.6	39.2	23.1	17.7	33.6	272	1.98	0.85	205	332	7.5
Max	5.59	89.6	122	40.4	126	81.7	415	30.3	2.99	825	718	8.3
Mean	2.92	60.57	71.09	31.77	56.72	61.16	348.8	7.76	1.45	324.9	492.57	7.92
SD	1.01	15.36	22.27	4.02	36.79	13.08	40.94	5.74	0.51	115.25	112.14	0.21
CV/%	34.53	25.36	31.33	12.66	64.86	21.38	11.74	73.97	34.92	35.47	22.77	2.64
CS ¹	/	200	/	/	250	250	/	20	/	/	1000	6.5–8.5
WG ²	/	200	/	/	250	500	/	50	/	/	1000	6.5–8.5

* TH is the total hardness, ¹ CS is the Chinese Standards, ² WG is the WHO Guidelines.

3.1.2. Hydrochemical Facies

Piper's trilinear diagram can be used to characterize the total chemical properties and major ionic composition changes of a water body [36,37]. As shown in Figure 2, the groundwater sample points were concentrated in zone 4 of the diamond-shaped domain of the Piper trilinear diagram, indicating that the chemistry of Sr-rich groundwater in the study area is dominated by alkaline earth metal elements (calcium and magnesium) rather than the alkali metal elements (sodium). On the other hand, the groundwater sample points were concentrated in the E region of the anion triangle of the Piper trilinear diagram, indicating the dominance of weak acidic anions (carbonic acid), whereas the observed cations were concentrated in the B region of the Piper trilinear diagram (cationic triangular domain), suggesting a non-dominant type. In general, the distribution of Sr-rich groundwater sampling sites in the study area was relatively concentrated, showing six main types, among which $\text{HCO}_3^- \text{Ca}\cdot\text{Mg}\cdot\text{Na}$ was the main groundwater facies type, accounting for 70% of the total groundwater samples, followed by $\text{HCO}_3^- \text{Ca}\cdot\text{Na}\cdot\text{Mg}$ and $\text{HCO}_3^- \text{Ca}\cdot\text{Mg}$ groundwater facies types, both accounting for 20% of the total groundwater samples, while $\text{HCO}_3^- \text{Na}\cdot\text{Mg}\cdot\text{Ca}$, $\text{HCO}_3^- \text{Mg}\cdot\text{Ca}\cdot\text{Na}$ and $\text{HCO}_3^- \text{Mg}\cdot\text{Na}\cdot\text{Ca}$ groundwater facies type were less abundant. In addition, TIS salinity diagram can further characterize the chemical composition of water [38]. As shown in Figure 3, $(\text{Cl}^- + \text{HCO}_3^-)$ content is $5.11\sim 10.21 \text{ meq}\cdot\text{L}^{-1}$, SO_4^{2-} content is $1.4\sim 3.6 \text{ meq}\cdot\text{L}^{-1}$. Indeed, the total ionic salinity (TIS) of water ranges from 14.2 to $26.4 \text{ meq}\cdot\text{L}^{-1}$. The strontium-rich groundwater has high TIS value, which indicates that the strontium-rich groundwater is the result of a long-term evolution of the groundwater system in the study area.

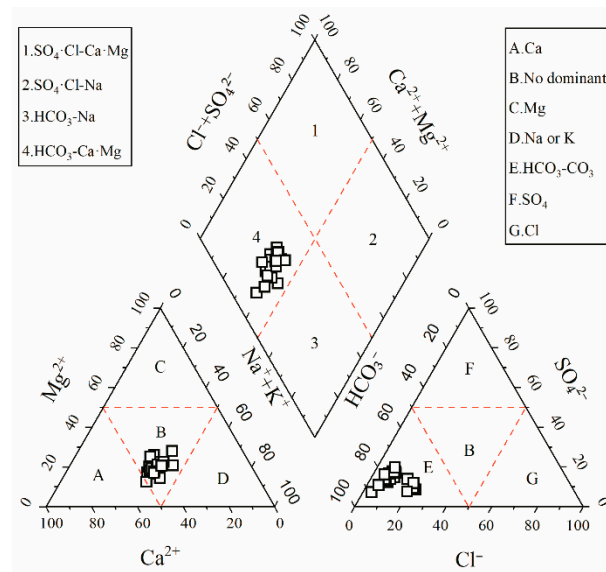


Figure 2. Piper trilinear diagram of Sr-rich groundwater.

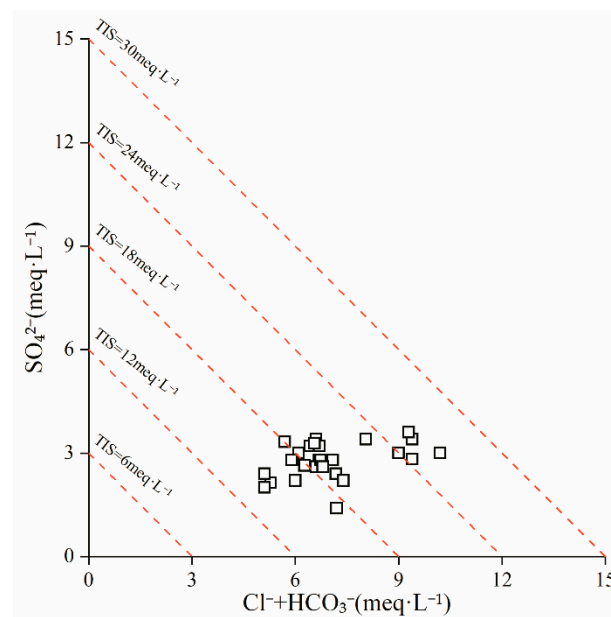


Figure 3. TIS salinity diagram of Sr-rich groundwater.

3.1.3. Correlation Analysis of Hydrochemical Compositions

Correlation analysis can reveal the consistency and variability of the sources of groundwater hydrochemical parameters. As shown in Figure 4, Cl^- showed a high positive correlation with Na^+ and Ca^{2+} and moderate correlation with Mg^{2+} , with correlation coefficients of 0.92, 0.94, and 0.59, respectively. HCO_3^- showed moderately positive correlations with Na^+ and Ca^{2+} , with correlation coefficients of 0.74 and 0.69, respectively, while SO_4^{2-} and NO_3^- revealed negative correlations with all cations in groundwater. NO_3^- showed a moderate negative correlation with K^+ , with a correlation coefficient of -0.56 . As for Cl^- , it showed a moderate positive correlation with HCO_3^- , with a correlation coefficient of 0.59. Sr^{2+} showed a high correlation with Na^+ and Cl^- , with correlation coefficients of 0.85 and 0.84, respectively, suggesting that the source of Sr in groundwater is closely related to the effect of atmospheric precipitation. In addition, Sr^{2+} revealed moderate positive correlations with Ca^{2+} and HCO_3^- , with correlation coefficients of 0.73 and 0.59, respectively, indicating that the source of Sr may be the same as these two ions. The correlation

between TDS and ions can better reflect the genesis of groundwater. Indeed, TDS showed positive correlation coefficients with Cl^- and Na^+ of 0.81 and 0.76, indicating high and moderate correlation, respectively, and an atmospheric precipitation source of groundwater. The correlation coefficients of TDS with Ca^{2+} and HCO_3^- were 0.84 and 0.60, showing high and moderate correlations, respectively, indicating that Ca^{2+} and HCO_3^- contribute significantly to the formation of groundwater chemistry types in the carbonate-rich rock study area.

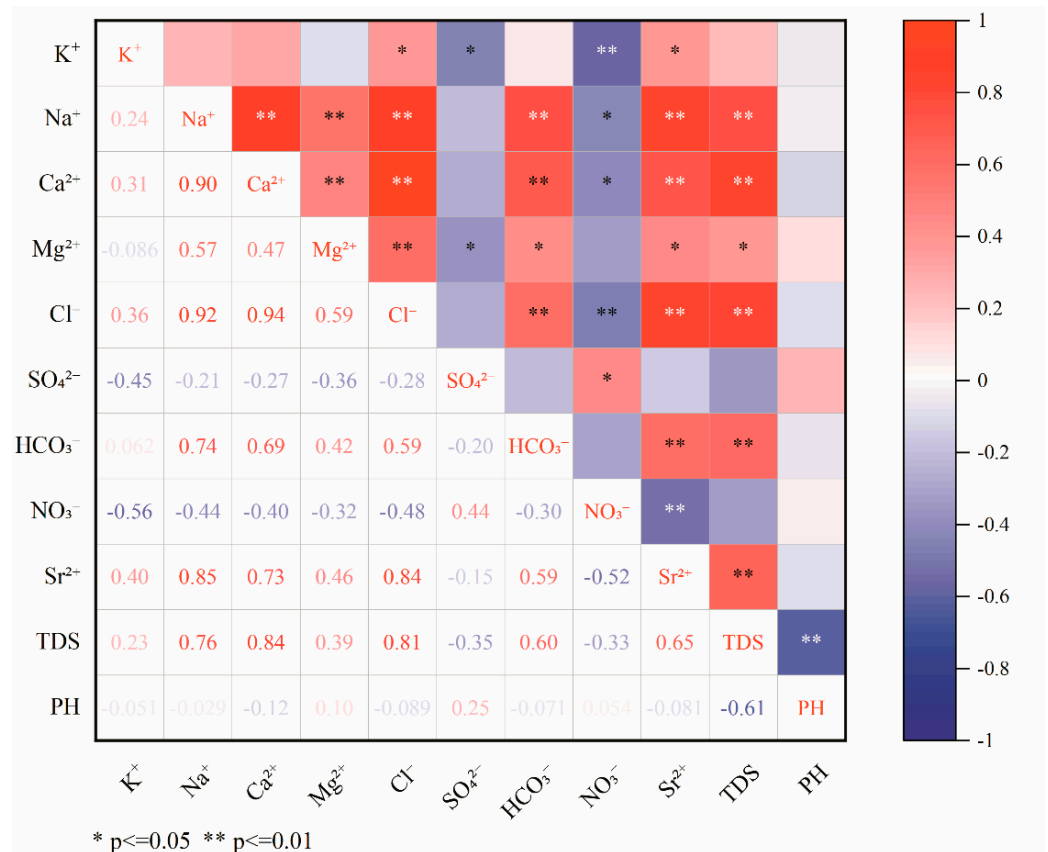


Figure 4. Correlation coefficients between hydrochemical parameters of Sr-rich groundwater.

3.1.4. Controlling Factors and Natural Processes

A Gibbs diagram is an important tool for analyzing the chemical genesis of water and can be used to analyze the mechanism of ion formation in water bodies [39,40]. In the Gibbs diagram, the ion control mechanism is classified into three main effects, namely rock weathering, evaporation-concentration, and atmospheric precipitation. The variation of $\text{Cl}^- / (\text{Cl}^- + \text{HCO}_3^-)$ and $\text{Na}^+ / (\text{Na}^+ + \text{Ca}^{2+})$ ratios in Sr-rich groundwater samples in the study area varied slightly from 0.04 to 0.25 and from 0.42 to 0.56, with mean values of 0.13 and 0.56, respectively. In addition, TDS values were at a moderate level, varying from 332 to 718 $\text{mg}\cdot\text{L}^{-1}$, with a mean value of 493 $\text{mg}\cdot\text{L}^{-1}$. As shown in Figure 5, the Sr-rich groundwater samples were mainly located in the rock weathering area of the Gibbs diagram, indicating that rock weathering was the most influential mechanism in the genesis of Sr-rich groundwater in the study area. In addition, some Sr-rich groundwater samples were close to the evaporation-concentration zone, indicating the slight influential effect of the evaporation-concentration process on the hydrochemical characteristics of Sr-rich groundwater in the study area. However, the groundwater samples were all far away from the atmospheric precipitation zone, suggesting the lack of any significant effect of atmospheric precipitation on the water chemistry of Sr-rich groundwater.

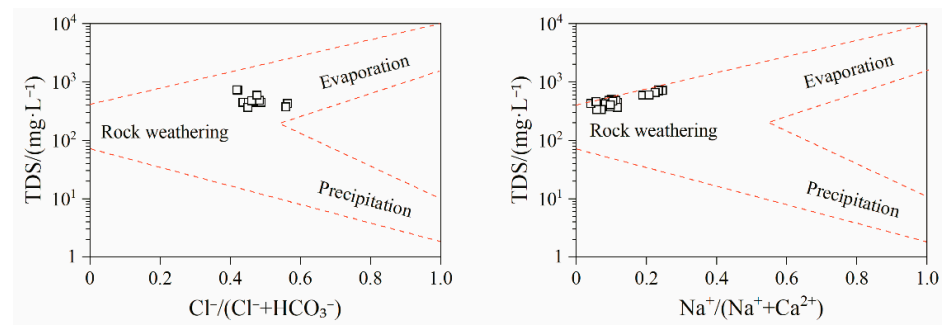


Figure 5. Gibbs plot of Sr-rich groundwater.

In this study, the direction and strength of the cation exchange interaction were assessed using the chloro-alkaline indices [41], namely CAI-I and CAI-II. These indices were calculated using the following formulas:

$$CAI - I = \frac{Cl^- - (Na^+ + K^+)}{Cl^-} \tag{1}$$

$$CAI - II = \frac{Cl^- - (Na^+ + K^+)}{HCO_3^- + SO_4^{2-} + CO_3^{2-} + NO_3^-} \tag{2}$$

When both CAI-I and CAI-II values are less than 0, it indicates that Ca^{2+} or Mg^{2+} in groundwater exchanged ions with Na^+ in aquifer minerals. When CAI-I and CAI-II values are greater than 0, it indicates that Na^+ in the groundwater exchanged ions with Ca^{2+} or Mg^{2+} in the aquifer minerals. In addition, the higher the absolute values of CAI-I and CAI-II the chloride index, the higher the degree of ion exchange.

The results showed that CAI-I and CAI-II varied from -0.23 to 0.01 and from -3.71 to 0.004 , with a mean value of -0.128 and -1.155 , respectively (Figure 6a). In addition, almost groundwater samples revealed negative values of chloro-alkaline indices, except for a few points. This result suggests that the cation exchange process generally occurs in groundwater in the study area, more specifically replacement of Na^+ with Ca^{2+} and Mg^{2+} from aquifer minerals to the groundwater. Except for a few samples, relatively high absolute values of the chloro-alkaline indices were observed in Sr-rich groundwater samples, suggesting a strong degree of cation exchange. A very small number of water samples do not undergo alternate cation adsorption, which may be due to the influence of some other sources. In addition, the relationship between $Na^+ + K^+$ and Cl^- can also be investigated to assess cation exchange. As shown in Figure 6b, the water samples were distributed above the $[(Na^+ + K^+) - Cl^-]$ ratio 1:1 line, indicating a significant enrichment of groundwater by $(Na^+ + K^+)$ compared to Cl^- . Indeed, except for rock salt and potassium salt dissolution, there are also other sources of Na^+ and K^+ , mainly due to the presence of a certain degree of cation exchange to increase the Na^+ content.

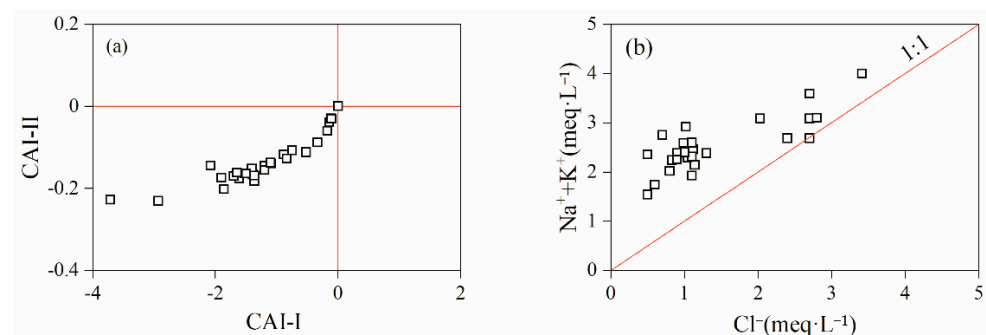


Figure 6. Chloro-alkaline indices (a) and the relationship between $Na^+ + K^+$ and Cl^- (b) in Sr-rich groundwater.

The mineral saturation index (SI) can be used to indicate the dissolved equilibrium state of groundwater components. The results showed positive values of saturation indices of dolomite, gypsum, and calcite (Table 2), indicating that all three minerals were in supersaturated states and were in sedimentation states during groundwater evolution. However, the saturation index range of rock salt in the study area was negative, indicating that the rock salt was in a dissolved state during groundwater evolution.

Table 2. Mineral saturation index in Sr-rich groundwater.

SI	Min	Max	Mean	SD
Dolomite	5.24	5.98	5.55	0.29
Gypsum	1.97	2.95	2.36	0.37
rock salt	−5.73	−3.92	−5.13	0.75
Calcite	4.53	4.92	4.71	0.14

3.1.5. Qualitative Analysis of Ion Sources

Water bodies are constantly interacting with the natural environment through various hydrogeochemical processes. In the process of groundwater circulation, hydrochemical ratios have a certain regularity, which can be used to assess the water chemistry and its main sources [42].

The Na^+/Cl^- ratio can characterize the degree of Na^+ enrichment in groundwater [43]. According to the correlation analysis (Figure 4), a high correlation was observed between Na^+ and Cl^- ($r = 0.92$). However, most of the water samples fall above the rock salt dissolution line (Figure 7a), with a Na^+/Cl^- ratio range of 0.96–4.58, with an average value of 2.09. The result showed a higher Na^+ enrichment compared to Cl^- , suggesting that Na^+ does not originate from the dissolution of rock salt only. Indeed, besides cation exchange that may increase the Na^+ content in Sr-rich groundwater in Tianjiazhai, the dissolution of silicate minerals (e.g., sodium feldspar) can contribute to the increase in Na^+ concentrations in groundwater.

$\text{Ca}^{2+}/\text{Mg}^{2+}$, $(\text{Ca}^{2+} + \text{Mg}^{2+})/\text{HCO}_3^-$, and $(\text{Ca}^{2+} + \text{Mg}^{2+})/(\text{HCO}_3^- + \text{SO}_4^{2-})$ ratios can be used to determine the sources of Ca^{2+} and Mg^{2+} in groundwater [44,45]. From Figure 7b, the results showed a $\text{Ca}^{2+}/\text{Mg}^{2+}$ ratio range of 0.33–1.05, with a mean value of 0.67. Except for a few samples located on the 1:1 line, most groundwater samples fell below the 1:1 line, indicating that the sources of Ca^{2+} and Mg^{2+} in the study area are calcite and dolomite dissolution; this is mainly due to the fact that calcite reached saturation faster than dolomite. As shown in Figure 7c, all groundwater samples fall above the 1:1 line of the $(\text{Ca}^{2+} + \text{Mg}^{2+})/\text{HCO}_3^-$ ratio. In addition, the results showed a $(\text{Ca}^{2+} + \text{Mg}^{2+})/\text{HCO}_3^-$ ratio range of 1.18–1.99, with an average value of 1.55, indicating that Ca^{2+} and Mg^{2+} were more enriched than HCO_3^- . This finding suggests that Ca^{2+} and Mg^{2+} were derived from the dissolution of carbonate rocks as well as from other sources, such as the dissolution of gypsum. In addition, most groundwater samples fall at the 1:1 line of the $[(\text{Ca}^{2+} + \text{Mg}^{2+})/(\text{HCO}_3^- + \text{SO}_4^{2-})]$ ratio (Figure 7d), which indicates equilibrium states of these ions, while chloro-alkaline indices indicated the prevalence of cation exchange. Moreover, this result demonstrates that Ca^{2+} and Mg^{2+} were not only from the dissolution of calcite, dolomite, and gypsum but also from silicate dissolution. $(\text{Ca}^{2+} + \text{Mg}^{2+})$ and $(\text{HCO}_3^- + \text{SO}_4^{2-})$ were in equilibrium under the combined influence of carbonate rock, silicate rock, and cation exchange.

Most of the groundwater samples fell near the 1:1 line of the $\text{Ca}^{2+}/\text{SO}_4^{2-}$ ratio (Figure 7e), while only a few samples fell below the 1:1 line, showing that most of the groundwater samples have relatively balanced Ca^{2+} and SO_4^{2-} , while a few samples are depleted in Ca^{2+} or enriched in SO_4^{2-} . This result may be due to the presence of a certain degree of cation exchange and sedimentation of carbonate rocks during the evolution of groundwater.

The relationship between the HCO_3^- and $(\text{SO}_4^{2-} + \text{Cl}^-)$ can further reflect the dissolved carbonate rock in groundwater. As shown in Figure 7f, the water samples fall above

the 1:1 line of the $\text{HCO}_3^- / (\text{SO}_4^{2-} + \text{Cl}^-)$ ratio. Moreover, the $\text{HCO}_3^- / (\text{SO}_4^{2-} + \text{Cl}^-)$ ratios range from 1.02 to 3.53, with an average value of 1.45. The HCO_3^- enrichment compared to $(\text{SO}_4^{2-} + \text{Cl}^-)$ indicated the dominance of HCO_3^- in Sr-rich groundwater in Tianjiazhai, suggesting that the water chemistry is mainly influenced by carbonate rock dissolution, which is consistent with the groundwater facies type.

The $\text{Cl}^- / \text{Na}^+$ and $\text{NO}_3^- / \text{Na}^+$ ratios in groundwater are generally higher when the groundwater is affected by anthropogenic activities [46]. The variation in the $\text{Cl}^- / \text{Na}^+$ and $\text{NO}_3^- / \text{Na}^+$ ratios in the Sr-rich groundwater samples in Tianjiazhai ranged from 0.22 to 1.04 and from 0 to 0.22, with mean values of 0.56 and 0.05, respectively. The low $\text{Cl}^- / \text{Na}^+$ and $\text{NO}_3^- / \text{Na}^+$ ratios obtained suggested that Sr-rich groundwater in Tianjiazhai is less affected by anthropogenic activities.

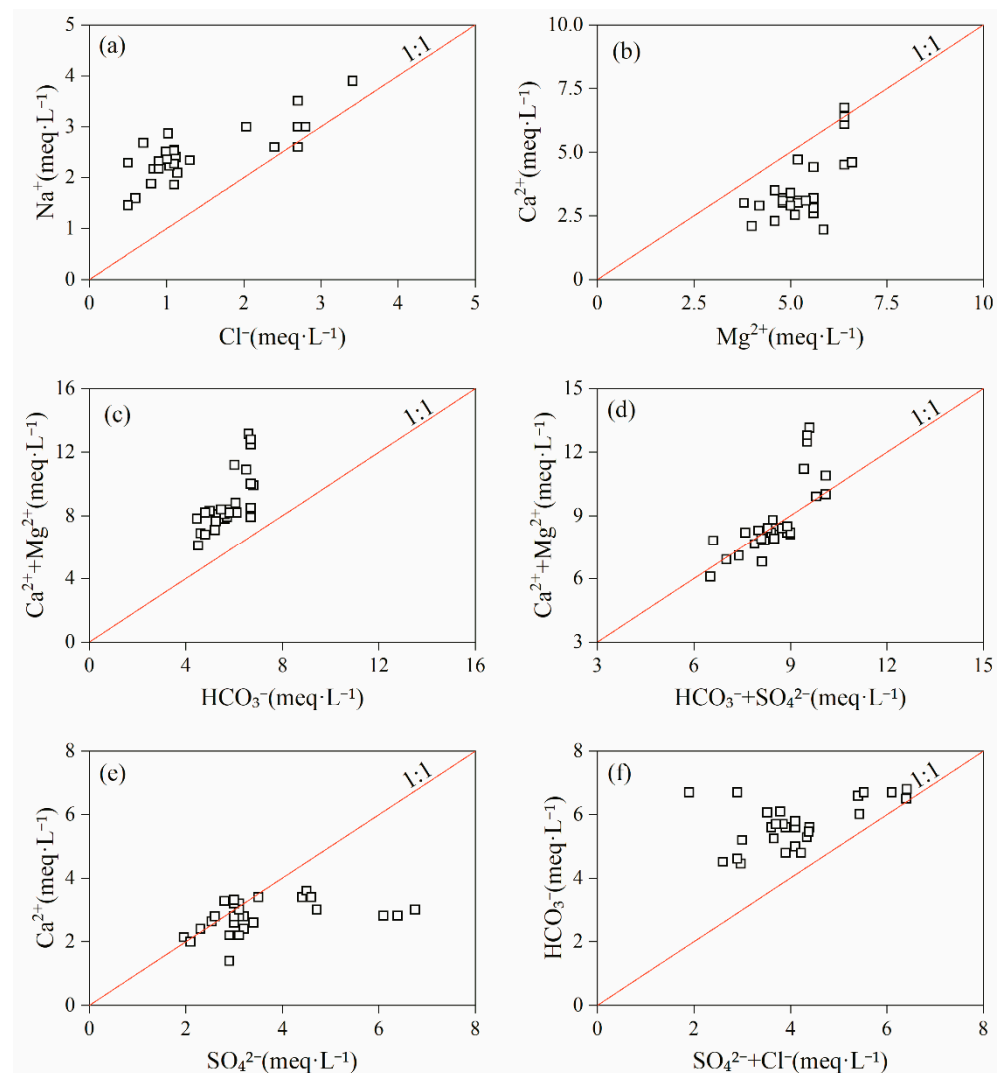


Figure 7. Relationship between the main ion ratios of Sr-rich groundwater. (a) Cl^- and Na^+ ; (b) Mg^{2+} and Ca^{2+} ; (c) HCO_3^- and $(\text{Ca}^{2+} + \text{Mg}^{2+})$; (d) $(\text{HCO}_3^- + \text{SO}_4^{2-})$ and $(\text{Ca}^{2+} + \text{Mg}^{2+})$; (e) SO_4^{2-} and Ca^{2+} ; (f) $(\text{SO}_4^{2-} + \text{Cl}^-)$ and HCO_3^- .

3.2. Formation Mechanism of Sr in Groundwater

3.2.1. Source Conditions

The upper part of the lithosphere is rich in trace elements, such as Sr, which is abundantly contained in most rocks [47]. Indeed, Sr is mostly distributed in rock-forming minerals and is relatively concentrated in amphibolites, granites, and carbonates [48]. The Sr content in the clastic rocks of the Yanchang Formation in the study area is high. In addition,

the lithology of this formation is a thick-bedded feldspathic sandstone of light gray-green medium to fine-grained feldspathic sandstone containing a large amount of potassium feldspar, which is rich in Sr. Strontium in groundwater is mainly derived from the dissolution of strontium in the sandstones of the Yanchang Formation. The Sr abundance in the surrounding rocks can reflect the Sr content in groundwater. Indeed, the presence of Sr-bearing minerals is the material basis for the formation of Sr-rich groundwater.

3.2.2. Hydrodynamic Conditions

The Sr-rich groundwater in Tianjiazhai is mainly stored in the fractured unconfined aquifer of the Yanchang Formation. The natural geographical, geological, and hydrogeological conditions in the area determine the alternating characteristics of the overall circulation of Sr-rich groundwater. During the rainy season, the main sources of recharge for weathered fractured unconfined water in the Yanchang Formation are atmospheric precipitation, Quaternary loose layer unconfined water, and surface water, while during the dry period, the weathered fractured unconfined water of the Yanchang Formation is mainly recharged from atmospheric precipitation and through transient runoff. Indeed, discharge occurs from high to low and from West to East, recharging surface water and pore unconfined water in the loose layer of the Quaternary, thus locally recharging the Shimachuan area through runoff, from upstream to downstream. The weathered fissure groundwater in the Yanchang Formation is located in different geomorphological units, resulting in different recharge modes, runoff directions, and discharge conditions. The Yanchang Formation of weathered fissure unconfined water, which is distributed in the Loess Mountains, mainly receives infiltration recharge from the overlying Quaternary aquifer and then flows from the Loess to the surrounding lowlands and discharges to the surface in the lowlands of the topographically cut gullies to recharge the weathered fissure groundwater of the Yanchang Formation in the river valley area. The weathered fractured groundwater of the Yanchang Formation, distributed in the valley area, mainly receives the recharge from the pore water of the overlying loose layer and the lateral recharge of the same aquifer. Besides the low recharge rates from the lower confined water, the exposed section of the aquifer is recharged directly from the atmospheric precipitation when the local section of the valley area is in the favorable part of the geomorphology before flowing along the river valley downstream from high to low elevations and from upstream to downstream areas. The discharge of the aquifer occurs in the form of submerged flow discharge in the riverbed, followed by downstream discharge. In addition, discharge by evaporation and artificial mining is also the main discharge process. There is no aquifuge between aquifers of the Quaternary loose layer pore unconfined water and the weathered fissure unconfined water of the Yanchang Formation, indicating a relatively close hydraulic connection. Surface water bodies and the Quaternary-Holocene alluvial unconfined water have a complementary relationship, resulting in the close relationship between weathered fissure unconfined water in the Yanchang Formation and surface water. According to the results of the dynamic surface water observation and groundwater level data observed from observation wells in Shimachuan, the dynamic changes of groundwater are closely related to atmospheric precipitation with the characteristics of synchronous changes. All this provides hydrodynamic conditions for the Sr enrichment in groundwater.

3.2.3. Hydrochemical Conditions

The Sr-rich groundwater in Tianjiazhai is mainly stored in the weathered fractured unconfined aquifer of the Yanchang Formation. Indeed, the rocks in the study area have a large weathering thickness and fracture development, mostly in the form of lines and veins and locally in the form of a network. Atmospheric precipitation recharges groundwater through fissure infiltration, resulting in CO₂ seepage into the ground with precipitation during the infiltration process (the free carbon dioxide in groundwater is determined by the volumetric method of standard base solution). Under certain temperature and pressure conditions, Sr-bearing minerals (rocks) undergo hydrolysis and dissolution filtration to form

Sr-rich groundwater. The thick layer of weathered rocks developed in the Tianjiazhai area, endowed with rich groundwater resources, provides good water conductivity channels and reaction space for groundwater circulation and water–rock interaction.

The Sr content in the upper and lower parts of Borehole G019 (Figure 8a) ranged from 0.14 to 0.20‰ and from 0.33 to 0.39‰, respectively. The Sr content in the upper and lower parts of borehole G020 (Figure 8b) ranged from 0.11 to 0.40‰ and from 0.51 to 0.62‰, respectively. The Sr contents of rock samples at different depths in the hydrogeological borehole were generally lower in the upper strata than in the lower strata. This result may be due to the higher weathering degree of the rocks in the upper strata than in the lower strata, resulting in high Sr element concentration, with high content, entering the groundwater. As can be seen from Table 3, Sr was prevalently present in the strata of the study area, ranging from 0.0741 to 0.147‰. By comparing the Sr content in the borehole and profile, lower Sr contents were observed in the profile than those in the borehole, which may be due to the longer leaching time in the area where the profile is located, allowing Sr to easily dissociate from rocks and enter groundwater. Therefore, the Sr enrichment in groundwater in Tianjiazhai is influenced by the degree of weathering and water–rock reaction time. The higher the degree of weathering and the longer the water–rock reaction time, the more easily Sr is leached from the rock into the groundwater system.

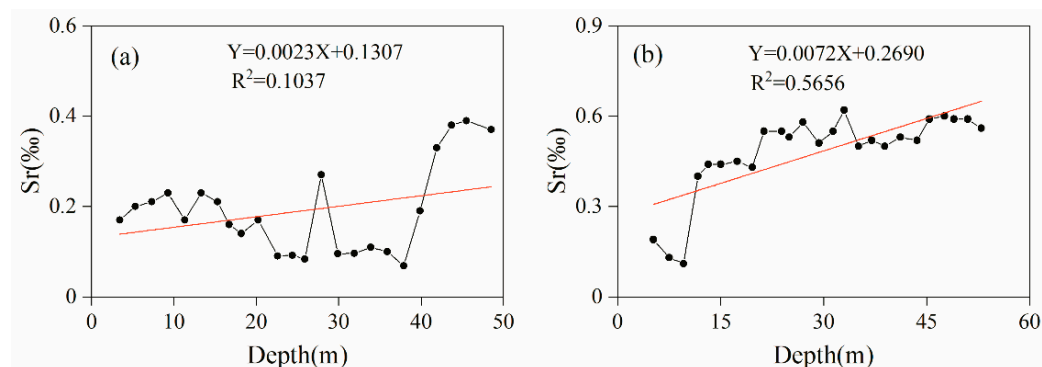


Figure 8. Sr content of strata in hydrogeological boreholes G019 (a) and G020 (b).

Table 3. Sr content in rock sample profiles.

Rock	Lithology	Strontium (‰)	Rock	Lithology	Strontium (‰)
pm-1	Medium-grained sandstone	0.126	pm-12	Fine-grained sandstone	0.080
pm-2	Conglomerate	0.103	pm-13	Mudstone	0.143
pm-3	Fine-grained sandstone	0.101	pm-14	Fine-grained sandstone	0.111
pm-4	Fine-grained sandstone	0.076	pm-15	Mudstone	0.110
pm-5	Coarse-grained sandstone	0.098	pm-16	Mudstone	0.074
pm-6	Coarse-grained sandstone	0.147	pm-17	Mudstone	0.128
pm-7	Coarse-grained sandstone	0.120	pm-18	Mudstone	0.119
pm-8	Fine-grained sandstone	0.116	pm-19	Fine-grained sandstone	0.126
pm-9	Fine-grained sandstone	0.145	pm-20	Fine-grained sandstone	0.121
pm-10	Fine-grained sandstone	0.111	pm-21	Loess	0.255
pm-11	Fine-grained sandstone	0.116	pm-22	Loess	0.266

Strontium enrichment in groundwater is related to groundwater circulation and transport characteristics. In groundwater flow systems, the farther the runoff distance, the longer the circulation path, the longer the retention time of groundwater in the aquifer, and the more favorable the dissolution and enrichment of strontium in groundwater [49–51]. The Sr-rich groundwater in Tianjiazhai is mainly stored in the weathered fractured aquifer of the Yanchang Formation, with a single water-bearing lithology and good groundwater circulation conditions. The Sr contents in the altered bedrock fracture water are relatively stable. In addition, the clastic rock layer is less permeable and provides a semi-closed/semi-

open groundwater environment, with slow groundwater runoff, long retention time, and sufficient water–rock interaction, resulting in dissolution and enrichment of Sr in the groundwater. Long-term contact between groundwater and surrounding Sr-bearing minerals (rocks) is the fundamental condition for the formation of Sr-rich groundwater. The longer the contact time between groundwater and Sr minerals (rocks), the higher the Sr content in the groundwater.

4. Conclusions

In this study, the hydrochemical characteristics and sources of Sr-rich groundwater in the Tianjiazhai area were analyzed using descriptive analysis, correlation analysis, Piper trilinear diagrams, Gibbs plots and ion ratios. In addition, the formation mechanisms of Sr in groundwater were discussed, taking into account the specific geological and hydrogeological conditions of the study area, as well as the hydrogeochemical theory. The results showed that:

- (1) Sr^{2+} content in Sr-rich groundwater ranged from 0.85 to 2.99 $\text{mg}\cdot\text{L}^{-1}$, with an average value of 1.45 $\text{mg}\cdot\text{L}^{-1}$, which was 7.25 times higher than the national limit value of Sr^{2+} content in natural mineral water for drinking (0.20 $\text{mg}\cdot\text{L}^{-1}$). In addition, the pH and TDS values ranged from 7.50 to 8.30 and from 332.00 to 718.00 $\text{mg}\cdot\text{L}^{-1}$, respectively, indicating that Sr-rich groundwater is generally slightly alkaline. The dominant cation and anion were Ca^{2+} and HCO_3^- , respectively. On the other hand, HCO_3^- - $\text{Ca}\cdot\text{Mg}\cdot\text{Na}$ was the main facies type of Sr-rich groundwater in the Tianjiazhai area. The coefficients of variation of the hydrochemical parameters of Sr-rich groundwater were less than 1, indicating that the contents of all hydrochemical parameters indicators were relatively stable.
- (2) The correlation coefficients of Sr^{2+} with Ca^{2+} and HCO_3^- were 0.73 and 0.59, respectively, indicating that the source of Sr may be the same as that of these two ions. The correlation coefficients of TDS with Cl^- and Na^+ were 0.81 and 0.76, respectively, mainly because that the groundwater in the Tianjiazhai area originated from atmospheric precipitation, whereas the correlation coefficients of TDS with Ca^{2+} and HCO_3^- were 0.84 and 0.60, respectively, indicating the important role of Ca^{2+} and HCO_3^- in the groundwater chemistry in the study area. The hydrochemical characteristics of Sr-rich groundwater in the Tianjiazhai area are controlled by water–rock interactions and influenced by cation exchange. In addition, water–rock interactions in Sr-rich groundwater are dominated by the dissolution of carbonate rocks.
- (3) Weathering, dissolution, and leaching in the sandstone of the Yanchang Formation are the main processes controlling Sr content in groundwater. Indeed, the Sr-rich groundwater is mainly stored in the weathering fracture unconfined aquifer of the Yanchang Formation. In addition, the higher the degree of weathering of Sr-bearing minerals (rocks) and the longer the reaction time of water–rock interaction, the more favorable the dissolution and enrichment of Sr in groundwater. The hydrogeological conditions and geological and tectonic environment of the Tianjiazhai area provide favorable conditions for the formation of Sr-rich groundwater.

The sandstone of Yanchang Formation is widely distributed in the Shimachuan River basin, and the hydrodynamic and hydrochemical conditions of Shimachuan River basin are conducive to the enrichment of strontium in groundwater, and the strontium in groundwater flowing into Yellow River will be more enriched. Therefore, the development of this study is of typical significance and can provide a scientific basis for the study of strontium-rich groundwater in the whole Shimachuan River basin. However, due to the special geological environment of the study area, soil erosion is more serious, the groundwater quality is poor in the downstream region, and the sediment content in the groundwater injected into the Yellow River is especially large. Therefore, the above changes should be further explored in future research.

This study provides a deeper understanding of the hydrochemical characteristics and sources of Sr-rich groundwater in the Tianjiazhai area. The results obtained can also

provide a scientific basis and theoretical guidance for the development, utilization, and protection of Sr-rich groundwater.

Author Contributions: Research conceptualization, C.L. and W.W.; data curation, D.W. and A.O.; methodology, C.L.; writing—original draft, C.L.; writing—review and editing, W.W. and X.K., supervision, W.W. All authors have read and agreed to the published version of the manuscript.

Funding: This research received no external funding.

Institutional Review Board Statement: Not applicable.

Informed Consent Statement: Not applicable.

Data Availability Statement: All processed data generated or used during the study appear in the submitted article. Raw data may be provided on reasonable request from the corresponding author.

Acknowledgments: We acknowledge the Shaanxi Province 139 Coal Geology and Hydrology Co. for the access to original information.

Conflicts of Interest: The authors declare no conflict of interest.

References

1. Karunanidhi, D.; Aravinthasamy, P.; Deepali, M.; Subramani, T.; Bellows, B.C.; Li, P. Groundwater quality evolution based on geochemical modeling and aptness testing for ingestion using entropy water quality and total hazard indexes in an urban-industrial area (Tiruppur) of Southern India. *Environ. Sci. Pollut. Res.* **2021**, *28*, 18523–18538. [[CrossRef](#)]
2. Li, P.; He, X.; Guo, W. Spatial groundwater quality and potential health risks due to nitrate ingestion through drinking water: A case study in Yan'an City on the Loess Plateau of northwest China. *Hum. Ecol. Risk Assess. Int. J.* **2019**, *25*, 11–31. [[CrossRef](#)]
3. Alvarez, M.d.P.; Funes, D.; Dapeña, C.; Bouza, P.J. Origin and hydrochemical characteristics of groundwater in the Northeastern Patagonia, Argentina: The relationship with geomorphology and soils. *Environ. Earth Sci.* **2020**, *79*, 503. [[CrossRef](#)]
4. Li, Y.; Li, P.; Cui, X.; He, S. Groundwater quality, health risk, and major influencing factors in the lower Beiluo River watershed of northwest China. *Hum. Ecol. Risk Assess. Int. J.* **2021**, *27*, 1987–2013. [[CrossRef](#)]
5. Srinivas, Y.; Aghil, T.B.; Hudson Oliver, D.; Nithya Nair, C.; Chandrasekar, N. Hydrochemical characteristics and quality assessment of groundwater along the Manavalakurichi coast, Tamil Nadu, India. *Appl. Water Sci.* **2017**, *7*, 1429–1438. [[CrossRef](#)]
6. Liu, J.; Gao, Z.; Wang, M.; Li, Y.; Shi, M.; Zhang, H.; Ma, Y. Hydrochemical characteristics and possible controls in the groundwater of the Yarlung Zangbo River Valley, China. *Environ. Earth Sci.* **2019**, *78*, 76. [[CrossRef](#)]
7. Chotpantarat, S.; Thamrongsrisakul, J. Natural and anthropogenic factors influencing hydrochemical characteristics and heavy metals in groundwater surrounding a gold mine, Thailand. *J. Asian Earth Sci.* **2021**, *211*, 104692. [[CrossRef](#)]
8. Feng, W.; Qian, H.; Xu, P.; Hou, K. Hydrochemical Characteristic of Groundwater and Its Impact on Crop Yields in the Baojixia Irrigation Area, China. *Water* **2020**, *12*, 1443. [[CrossRef](#)]
9. Bowman, R.S. Aqueous Environmental Geochemistry. *Eos Trans. Am. Geophys. Union* **1997**, *78*, 586. [[CrossRef](#)]
10. Fuoco, I.; De Rosa, R.; Barca, D.; Figoli, A.; Gabriele, B.; Apollaro, C. Arsenic polluted waters: Application of geochemical modelling as a tool to understand the release and fate of the pollutant in crystalline aquifers. *J. Environ. Manag.* **2022**, *301*, 113796. [[CrossRef](#)]
11. Fuoco, I.; Marini, L.; De Rosa, R.; Figoli, A.; Gabriele, B.; Apollaro, C. Use of reaction path modelling to investigate the evolution of water chemistry in shallow to deep crystalline aquifers with a special focus on fluoride. *Sci. Total Environ.* **2022**, *830*, 154566. [[CrossRef](#)]
12. Yang, F.; Liu, S.; Jia, C.; Gao, M.; Chang, W.; Wang, Y. Hydrochemical characteristics and functions of groundwater in southern Laizhou Bay based on the multivariate statistical analysis approach. *Estuar. Coast. Shelf Sci.* **2021**, *250*, 107153. [[CrossRef](#)]
13. Van Geldern, R.; Schulte, P.; Mader, M.; Baier, A.; Barth, J.A.C.; Juhlke, T.R.; Lee, K. Insights into agricultural influences and weathering processes from major ion patterns. *Hydrol. Processes* **2018**, *32*, 891–903. [[CrossRef](#)]
14. Ismail, E.; Abdelhalim, A.; Heleika, M.A. Hydrochemical characteristics and quality assessment of groundwater aquifers northwest of Assiut district, Egypt. *J. Afr. Earth Sci.* **2021**, *181*, 104260. [[CrossRef](#)]
15. Zhang, B.; Zhao, D.; Zhou, P.; Qu, S.; Liao, F.; Wang, G. Hydrochemical Characteristics of Groundwater and Dominant Water–Rock Interactions in the Delingha Area, Qaidam Basin, Northwest China. *Water* **2020**, *12*, 836. [[CrossRef](#)]
16. Dai, L.L.; Mei, M.L.; Chu, C.H.; Lo, E.C.M. Remineralizing effect of a new strontium-doped bioactive glass and fluoride on demineralized enamel and dentine. *J. Dent.* **2021**, *108*, 103633. [[CrossRef](#)]
17. Neves, N.; Campos, B.B.; Almeida, I.F.; Costa, P.C.; Cabral, A.T.; Barbosa, M.A.; Ribeiro, C.C. Strontium-rich injectable hybrid system for bone regeneration. *Mater. Sci. Eng. C* **2016**, *59*, 818–827. [[CrossRef](#)]
18. Haixue, L.; Xuxue, C.; Yuekun, M.; Weipo, L.; Bin, Z. Characteristics and formation mechanism of strontium-rich groundwater in Malian River drainage basin, Southern Ordos Basin. *Geoscience* **2021**, *35*, 682.
19. Wang, R.; Wu, X.; Zhai, Y.; Su, Y.; Liu, C. An Experimental Study on the Sources of Strontium in Mineral Water and General Rules of Its Dissolution—A Case Study of Chengde, Hebei. *Water* **2021**, *13*, 699. [[CrossRef](#)]

20. Cao, Y.; Song, L.; Liu, L.; Zhu, W.; Cui, S.; Wang, Y.; Guo, P. Preliminary study on strontium-rich characteristics of shallow groundwater in Dingtao area, China. *J. Groundw. Sci. Eng.* **2020**, *8*, 244–258.
21. Pit'eva, K.E.; Fortygina, M.A.; Mikheev, A.V. Formation of the composition and quality of carbonate mineral water of the Elburgan water bearing complex (Essentuki Town). *Mosc. Univ. Geol. Bull.* **2007**, *62*, 277–285. [[CrossRef](#)]
22. Lu, S.; Zhou, H.; Liu, W.; Chen, Q.; Yan, Z.; Chen, L. Distribution and enrichment of strontium in the Zigui karst watershed. *Geol. China* **2021**, *48*, 1865–1874.
23. Zuo, R.; Teng, Y.; Wang, J. Modeling migration of strontium in sand and gravel aquifer in the candidate VLLW disposal site. *J. Radioanal. Nucl. Chem.* **2009**, *281*, 653. [[CrossRef](#)]
24. Zhu, X.; Liu, W.; Li, Z.; Chen, T.; Ren, Y.; Shao, H.; Wang, L. Distribution and characterization analyses of strontium-bearing mineral spring water in the Chengde region. *Hydrogeol. Eng. Geol.* **2020**, *47*, 65–73.
25. Li, D.; Gan, S.; Li, J.; Dong, Z.; Long, Q.; Qiu, S.; Zhou, Y.; Lu, C. Hydrochemical characteristics and formation mechanism of strontium-rich groundwater in Shijiazhuang, north China plain. *J. Chem.* **2021**, *2021*, 5547924. [[CrossRef](#)]
26. Yang, Y.; Shao, C.; Lu, T.; Zhang, A. Discovery of Strontium-rich mineral water in Tingsiqiao and Guantangyi Town, Xianning. *Geol. China* **2021**, *48*, 1661–1662.
27. Li, P.; He, S.; Yang, N.; Xiang, G. Groundwater quality assessment for domestic and agricultural purposes in Yan'an City, northwest China: Implications to sustainable groundwater quality management on the Loess Plateau. *Environ. Earth Sci.* **2018**, *77*, 775. [[CrossRef](#)]
28. Xu, P.; Zhang, Q.; Qian, H.; Li, M.; Hou, K. Characterization of geothermal water in the piedmont region of Qinling Mountains and Lantian-Bahe Group in Guanzhong Basin, China. *Environ. Earth Sci.* **2019**, *78*, 442. [[CrossRef](#)]
29. Chung, S.Y.; Rajendran, R.; Senapathi, V.; Sekar, S.; Ranganathan, P.C.; Oh, Y.Y.; Elzain, H.E. Processes and characteristics of hydrogeochemical variations between unconfined and confined aquifer systems: A case study of the Nakdong River Basin in Busan City, Korea. *Environ. Sci. Pollut. Res.* **2020**, *27*, 10087–10102. [[CrossRef](#)]
30. Li, P.; He, S.; He, X.; Tian, R. Seasonal Hydrochemical Characterization and Groundwater Quality Delineation Based on Matter Element Extension Analysis in a Paper Wastewater Irrigation Area, Northwest China. *Expo. Health* **2018**, *10*, 241–258. [[CrossRef](#)]
31. Kwon, E.; Park, J.; Lee, J.M.; Kim, Y.-T.; Woo, N.C. Spatiotemporal changes in hydrogeochemistry of coastal groundwater through the construction of underground disposal facility for low and intermediate level radioactive wastes in Korea. *J. Hydrol.* **2020**, *584*, 124750. [[CrossRef](#)]
32. Su, C.; Huang, C.; Zou, S.; Xie, D.; Zhao, G.; Tang, J.; Luo, F.; Yang, Y. Enrichment environment and sources of strontium of groundwater in Xintian county, Hunan Province. *Carsologica Sin.* **2017**, *36*, 678–683.
33. Zhou, C.; Zou, S.; Xia, R.; Xue, Q.; Zhu, D.; Li, L.; Cao, J.; Li, J.; Xie, H. Extreme enrichment of strontium discovered in surface water and groundwater in the Guanling area of Guizhou Province. *Geol. China* **2021**, *48*, 961–962.
34. Zhang, Q.; Qian, H.; Xu, P.; Li, W.; Feng, W.; Liu, R. Effect of hydrogeological conditions on groundwater nitrate pollution and human health risk assessment of nitrate in Jiaokou Irrigation District. *J. Clean. Prod.* **2021**, *298*, 126783. [[CrossRef](#)]
35. Zhang, J.; Shi, Z.; Wang, G.; Jiang, J.; Yang, B. Hydrochemical characteristics and evolution of groundwater in the Dachaidan area, Qaidam Basin. *Earth Sci. Front.* **2021**, *28*, 194–205.
36. Piper, A. A Graphic Procedure in the Geochemical Interpretation of Water-Analyses. *Eos Trans. Am. Geophys. Union* **1944**, *25*, 914–923. [[CrossRef](#)]
37. He, X.; Li, P.; Wu, J.; Wei, M.; Ren, X.; Wang, D. Poor groundwater quality and high potential health risks in the Datong Basin, northern China: Research from published data. *Environ. Geochem. Health* **2021**, *43*, 791–812. [[CrossRef](#)]
38. Apollaro, C.; Di Curzio, D.; Fuoco, I.; Buccianti, A.; Dinelli, E.; Vespasiano, G.; Castrignanò, A.; Rusi, S.; Barca, D.; Figoli, A.; et al. A multivariate non-parametric approach for estimating probability of exceeding the local natural background level of arsenic in the aquifers of Calabria region (Southern Italy). *Sci. Total Environ.* **2022**, *806*, 150345. [[CrossRef](#)]
39. Marghade, D.; Malpe, D.B.; Duraisamy, K.; Patil, P.D.; Li, P. Hydrogeochemical evaluation, suitability, and health risk assessment of groundwater in the watershed of Godavari basin, Maharashtra, Central India. *Environ. Sci. Pollut. Res.* **2021**, *28*, 18471–18494. [[CrossRef](#)]
40. Gibbs Ronald, J. Mechanisms Controlling World Water Chemistry. *Science* **1970**, *170*, 1088–1090. [[CrossRef](#)]
41. Schoeller, H. Qualitative Evaluation of Groundwater Resources. In *Methods and Techniques of Groundwater Investigation and Development*; UNESCO: Paris, France, 1967.
42. Xing, L.; Guo, H.; Zhan, Y. Groundwater hydrochemical characteristics and processes along flow paths in the North China Plain. *J. Asian Earth Sci.* **2013**, *70–71*, 250–264. [[CrossRef](#)]
43. Zhao, Q.; Su, X.; Kang, B.; Zhang, Y.; Wu, X.; Liu, M. A hydrogeochemistry and multi-isotope (Sr, O, H, and C) study of groundwater salinity origin and hydrogeochemical processes in the shallow confined aquifer of northern Yangtze River downstream coastal plain, China. *Appl. Geochem.* **2017**, *86*, 49–58. [[CrossRef](#)]
44. Ma, R.; Wang, Y.; Sun, Z.; Zheng, C.; Ma, T.; Prommer, H. Geochemical evolution of groundwater in carbonate aquifers in Taiyuan, northern China. *Appl. Geochem.* **2011**, *26*, 884–897. [[CrossRef](#)]
45. Li, C.; Gao, X.; Wang, Y. Hydrogeochemistry of high-fluoride groundwater at Yuncheng Basin, northern China. *Sci. Total Environ.* **2015**, *508*, 155–165. [[CrossRef](#)]

46. Fan, B.-L.; Zhao, Z.-Q.; Tao, F.-X.; Liu, B.-J.; Tao, Z.-H.; Gao, S.; Zhang, L.-H. Characteristics of carbonate, evaporite and silicate weathering in Huanghe River basin: A comparison among the upstream, midstream and downstream. *J. Asian Earth Sci.* **2014**, *96*, 17–26. [[CrossRef](#)]
47. Ehya, F.; Shakouri, B.; Rafi, M. Geology, mineralogy, and isotope (Sr, S) geochemistry of the Likak celestite deposit, SW Iran. *Carbonates Evaporites* **2013**, *28*, 419–431. [[CrossRef](#)]
48. Parisi, S.; Paternoster, M.; Perri, F.; Mongelli, G. Source and mobility of minor and trace elements in a volcanic aquifer system: Mt. Vulture (southern Italy). *J. Geochem. Explor.* **2011**, *110*, 233–244. [[CrossRef](#)]
49. Zhang, Y.; Ding, H.; Fu, D.; Huang, Z.; Li, A.; Yan, C.; Jin, X. A study of enrichment environment and formation mechanism of strontium mineral water in Gansu Province. *Geol. China* **2020**, *47*, 1688–1701.
50. Su, C.; Nie, F.; Zou, S.; Zhao, G.; Luo, F.; Huang, Q.; Ba, J.; Li, X.; Liang, J.; Yang, Y. Hydrochemical Characteristics and Formation Mechanism of Strontium-rich Groundwater in Xintian County, Hunan Province. *Geoscience* **2018**, *32*, 554–564.
51. Sun, Q.; Sun, Z.; Jia, L.; Tian, H.; Guo, X.; Du, J.; Li, X.; Li, X.; Jia, L. Formation mechanism of the strontium-rich and metasilicic acid groundwater in the Lianhuashan area, Changchun, Jilin Province. *Geol. China* **2020**, *44*, 1031–1032.